Comparing Dry and Wet High-Intensity Magnetic Separation for Iron Removal from Low-Grade Magnesite Ore

Mohammed S. Alhaddad and Hussin A. M. Ahmed*
Mining Engineering Department, King Abdulaziz University, Jeddah, Saudi Arabia;

Comparación de la separación magnética de alta intensidad seca y húmeda para la eliminación de hierro de mineral de magnesita de bajo grado

Comparació de la separació magnètica d'alta intensitat seca i humida per a l'eliminació del ferro del mineral de magnesita de baix grau

RECEIVED: 13 JUNE 2024; ACCEPTED: 2 DECEMBER 2024 DOI: HTTPS://DOI.ORG/10.55815/432102

ABSTRACT

This paper investigates the removal of iron impurities from a low-grade Saudi magnesite ore (37.68% MgO and 1.91% Fe_2O_3). Both wet and dry high-intensity magnetic separation techniques were explored. In dry magnetic separation using an Outotec-induced roll magnetic, the feed size, feed rate, magnetic field, and roll speed were optimized. On the other hand, using a WHIMS laboratory wet high magnetic separator, the studied parameters were slurry flow rate, magnetic field, and pulp density. The results show that a maximum iron removal of 72.32% can be achieved using DHIMS (product with 0.71% Fe_2O_3 at (-0.212+0.05 mm) feed size, 0.3 kg/min feed rate, 14 KGauss, and a roll speed of 50 rpm. However, the optimal conditions for wet magnetic separation were magnetic field of 14 KGauss, 15 wt.% solid feed, and flow rate of 0.4 L/min, lead to a product that has 0.46% Fe_2O_3 which mean an iron removal of 84.25%. The product can be used in refractory materials, brake lining, leather treatment, and welding. It is also suitable for chemical, fertilizer, and wastewater treatment, flue gas treatment, and pesticides.

Keywords: magnesite, refractory, iron removal, Magnetic separation

RESUMEN

Este artículo investiga la eliminación de impurezas de hierro de un mineral de magnesita saudita de baja ley (37,68% MgO y 1,91% Fe2O3). Se exploraron técnicas de separación magnética de alta intensidad tanto húmedas como secas. En la separación magnética seca utilizando un rodillo magnético inducido por Outotec, se optimizaron el tamaño de alimentación, la velocidad de alimentación, el campo magnético y la velocidad del rodillo. Por otro lado, utilizando un separador magnético húmedo de laboratorio WHIMS, los parámetros estudiados fueron el caudal de la pulpa, el campo magnético y la densidad de la pulpa. Los resultados muestran que se puede lograr una eliminación máxima de hierro del 72,32% utilizando DHIMS (producto con 0,71% de Fe2O3 con un tamaño de alimentación (-0,212+0,05 mm), velocidad de alimentación de 0,3 kg/min, 14 kgauss y una velocidad de rodillo de 50 rpm. Sin embargo, las condiciones óptimas para la separación magnética húmeda fueron un campo magnético de 14 kgauss, 15% en peso de alimentación sólida y un caudal de . 0,4 L/min, dando como resultado un producto que tiene 0,46% Fe2O3 lo que significa una remoción de hierro del 84,25%. El producto puede ser utilizado en materiales refractarios, forros de frenos, tratamiento de cuero y soldadura. y tratamiento de aguas residuales, tratamiento de gases de combustión y pesticidas.

Palabra clave*:* magnesita, refractario, desferrizado, separación magnética

***Corresponding author: haahmed@kau.edu.sa**

RESUM

Aquest article investiga l'eliminació d'impureses de ferro d'un mineral de magnesita saudita de baix grau (37,68% MgO i 1,91% Fe2O3). Es van explorar tècniques de separació magnètica d'alta intensitat tant humida com seca. En la separació magnètica en sec mitjançant un magnètic de rotlle induït per Outotec, es van optimitzar la mida d'alimentació, la velocitat d'alimentació, el camp magnètic i la velocitat del rotllo. D'altra banda, utilitzant un separador magnètic alt humit de laboratori WHIMS, els paràmetres estudiats van ser el cabal de purins, el camp magnètic i la densitat de la polpa. Els resultats mostren que es pot aconseguir una eliminació màxima de ferro del 72,32% utilitzant DHIMS (producte amb 0,71% de Fe2O3 a (-0,212 + 0,05 mm) mida d'alimentació, velocitat d'alimentació de 0,3 kg/min, 14 KGauss i una velocitat de rotllo de 50 rpm. Tanmateix, les condicions òptimes per a la separació magnètica humida eren un camp magnètic de 14 KGauss, 15 % en pes d'alimentació sòlida i un cabal de 0,4 L/min, donen lloc a un producte que té un 0,46% de Fe2O3, la qual cosa significa una eliminació de ferro del 84,25%. També és adequat per al tractament de productes químics, fertilitzants i aigües residuals, tractament de gasos de combustió i pesticides.

Paraules clau*:* magnesita, refractari, eliminació de ferro, separació magnètica

1. INTRODUCTION

Magnesite is a mineral that falls under the calcite group and is commonly found in sedimentary and igneous rocks. The magnesite was once a primary source of magnesia, but now the magnesia can also be sourced from dolomite, olivine, brucite, and sea salts (Li et al., 2020). The primary component of magnesite is magnesium carbonate, which has a chemical formula of ($MgCO_3$). It comprises 47.6% magnesia (MgO) and 52.4% carbon dioxide (CO_2) by chemical weight. However, the natural state of magnesite can vary in composition due to impurities (Chatterjee, 2013; Shand, 2006).

Magnesite is a versatile mineral that finds application across diverse industrial sectors. It serves as a raw material for manufacturing a range of chemicals and intermediate products, such as Dead-Burned Magnesia (DBM) and Fused Magnesia (FM), which are used mainly in the refractory industry. Magnesia refractories are referred to as a basic refractory type with high refractoriness, because of the high melting point of MgO (2850 ^{0}C). These refractories are recognized for their exceptional ability to resist corrosion from basic steel-making slags (Biswas & Sarkar, 2020). The usage of magnesia refractories has significantly increased, especially for DBM, which constitutes 90% of total consumption (Chatterjee, 2013). Steel furnaces are the primary consumers of up to 70% of DBM. Following them are the lime and cement furnaces, which account for 7% of the total usage. The ceramics, glass, and chemical industries also use approximately 6% of DBM. The remaining percentage is utilized for other purposes (Kandianis & Kandianis, 2002). The classification of DBM is determined based on the iron content and CaO/SiO_2 ratio present in the brick composition. For high-performance commercial-grade MgO brick, a minimum of 80 wt.% of MgO is demanded (Biswas & Sarkar, 2020).

The high performance of magnesia's refractory material has excellent durability and high purity, achieved by low impurities constituting less than 10% of the material (Hou et al., 2020). These impurities in magnesite ore can be classified into two categories based on their mineral composition. The first group of impurities, called carbonate, includes minerals like calcite, dolomite, and rhodochrosite (Kim et al., 2018). The second group, silicate, comprises minerals such as quartz, talc, and serpentine. The presence of impurities in magnesite ore can have a significant impact on the quality of the intermediate products (DBM, FM) (Wang et al., 2011). The main effects are the appearance of cracks and a decrease in the melting point (Chatterjee, 2009). The reason for these effects can be related to the iron content and $CaO\text{-}MgO\text{-}SiO_2$ phases, which can be understood by referring to the typical analysis of the ternary $CaO\text{-}MgO\text{-}SiO_2$ phase diagram as shown in **Figure 1** (Jung et al., 2005; Rudnykh et al., 1988). The initial melting point of these phases is directly affected by the ratio of CaO to SiO_2, as shown in **Table 1**. When the CaO/SiO_2 ratio is greater than 2, the two phases of calcium-ferrite ($CaO.Fe_2O_3$) (C2F) and magnesium-ferrite spinel ($MgO.Fe_2O_3$) are formed. The iron impurities react with CaO and MgO to form calcium-ferrite and magnesium-ferrite spinel, respectively. These compounds lower the initial melting point, particularly in the first phase. Moreover, slag formation can be significantly influenced by high concentrations of iron impurities (Dippenaar, 2005). In the presence of these impurities, it also can be challenging to process magnesite during firing. Therefore, keeping impurities concentration at lower levels is essential (Chatterjee, 2009).

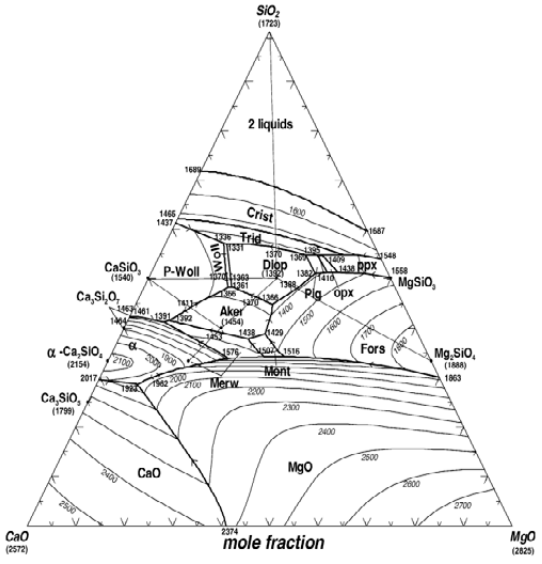

Figure 1. *CaO-MgO-SiO_2 phase diagram (Jung et al., 2005)*

Table 1. *The impact of Magnesite impurities on its initial melting point.*

CaO/ SiO2 ratio	Present Phase	Initial melting point (°C)	Reference
>2	calcium-ferrite (CaO. Fe_2O_3) (C2F) / magnesium ferrite spinel (Mg. Fe_2O_3)	1438 / 1716	(Wu et al., 2020; Xue et al., 2017)
=2.8	tricalcium silicate (Ca_3SiO_5)	-	(Biswas & Sarkar, 2020)
>2.8	tricalcium silicate (Ca_3SiO_5) / Calcium oxide (CaO)	1850	(Biswas & Sarkar, 2020)
2.8< CaO/ SiO2<1.87	tricalcium silicate (Ca_3SiO_5) / dicalcium silicate (Ca_2SiO_4)	1790	(Biswas & Sarkar, 2020)
=1.87	dicalcium silicate (Ca_2SiO_4)	-	(Biswas & Sarkar, 2020)
1.87< CaO/ SiO2<1.4	dicalcium silicate (Ca_2SiO_4) / merwinite ($Ca_3MgSi_2O_8$)	1575	(Biswas & Sarkar, 2020)
1.4< CaO/ SiO2<0.93	merwinite ($Ca_3MgSi_2O_8$) / monticellite ($CaMgSiO_4$)	1490	(Biswas & Sarkar, 2020)
<0.93	monticellite ($CaMgSiO_4$) / forsterite (Mg_2SiO_4)	1500	(Biswas & Sarkar, 2020)

Magnetic separation is a process to improve the quality of various industrial minerals. Its primary purpose is to remove iron-containing minerals and compounds, which can significantly enhance the final product's quality and purity (Atasoy, 2019). Magnesite is a mineral widely known for its diamagnetism property, meaning it has no magnetic properties. Magnesite's distinct magnetic susceptibility, ranging from (-6.4 to 45) × 10−9 m3/kg (Ishihara et al., 1987). However, magnesite, a naturally occurring mineral, can exhibit varying magnetic properties due to trace amounts of paramagnetic and ferromagnetic impurities. The magnetic properties of magnesite can be influenced by several impurities, such as magnetite, hematite, and goethite, which have high magnetic susceptibility (Yehia & Al-Wakeel, 2000).

Several research studies have been carried out to evaluate the efficiency of magnetic separation in magnesite beneficiation. Researchers like Suvorova et al. and Yehia and Al-Wakeel have utilized dry magnetic separation techniques to enhance magnesite ore quality by reducing impurities (Suvorova et al., 1984; Yehia & Al-Wakeel, 2013). In addition, Ignjatović et al. implemented a two-stage physical separation process involving heavy medium separation followed by wet magnetic separation (Ignjatović et al., 1995). Also, Bentli et al. and Hredzak et al. employed a magnetic separation technique to purify calcined magnesite ore by removing impurities (Bentli et al., 2017; Hredzak et al., 2015). Finally, Atasoy employed a wet magnetic separation technique to enhance the quality of magnesite ore waste (Atasoy, 2019). Until today, no investigation has been conducted on the enrichment of Saudi Arabia's low-grade magnesite ore. This study examines the iron impurities in the magnesite ore and optimizes the dry and wet magnetic separation conditions. Our primary objective was to use magnetic separation to obtain a magnesite product with a low Fe_2O_3 content suitable for use in the refractory industry.

2. MATERIAL AND METHODS

2.1 Materials

A representative sample of magnesite weighing 250 kg was obtained from the Al Ghazala mine, also known as the Zarghat project, in the Hail region of northwest Saudi Arabia. To ensure sample integrity, the magnesite was stored in dry bags to prevent moisture absorption. The rock material was first crushed using a laboratory jaw crusher and then ground by a ball mill, and the mill product was sieved at sizing screens ranging from -0.63 mm to 0 mm.

2.2 Methods

2.2.1 Sample preparation and characterization

The magnesite's microstructure, morphology, and composition were analyzed using Scanning Electron Microscopy (SEM). The elemental composition was determined through X-ray fluorescence (XRF). Additionally, the analysis was conducted to determine the presence of iron impurities for each size fraction. This analysis was also performed on each tested parameter's for feed and non-magnetic product. The experimental parameters for magnesite concentration were established based on prior research and subsequently modified to reflect the optimal findings or retained (Atasoy, 2019; Bentli et al., 2017; Hredzak et al., 2015; Ignjatović et al., 1995; Suvorova et al., 1984; Yehia & Al-Wakeel, 2013).

2.2.2 Dry high-intensity magnetic separator

The dry high-intensity magnetic separator, Outotec-induced roll MIH (13) 111-5 model, has been utilized in this study. The initial test conditions were set at a feed rate of 0.6 kg/min, a roll speed of 40 rpm, and a magnetic field intensity of 12000 Gauss. The magnesite feed size (-0.63+0.05, -0.425+0.05, -0.212+ 0.05, -0.1+0.05 mm) was initially tested. Afterward, the parameters that impact the separation procedure were adjusted and tested. These parameters include the feed rate (0.3, 0.9, 1.2 kg/min), magnetic field intensity (8K, 10K, 14K

Gauss), and roll speed (30, 50, 60 rpm). The magnetic field intensity was measured using a Gauss meter model (WT10A), while fractions were fully dried for one day at 105°C to guarantee complete dryness. A sample of 50 g was taken for each test, and the weights of the magnetic and non-magnetic fractions were recorded.

2.2.3 Wet high-intensity magnetic separator

The WHIMS 3X4L laboratory wet high magnetic separator was used in an experiment to determine the optimal conditions for the magnetic separation process. The initial conditions involved the feed size (-0.212+0.05mm), magnetic field intensity of 12000 Gauss, and a pulp density of 10 wt.% solid. The primary parameters influencing the separation process, including flow rate, magnetic field intensity, and pulp density, were tested at different levels. Specifically, the tests were conducted at flow rates (0.4, 0.8, 1.2, 1.6 L/min), magnetic field intensity (8K, 10K, 14K Gauss), and pulp density (5, 15, 20%). A Gauss meter model (WT10A) measured the magnetic field intensity. A sample of 50 g was taken for each test, and the weights of the magnetic and non-magnetic fractions were recorded.

3. RESULTS AND DISCUSSIONS

3.1 Low-grade magnesite ore characterization

Figure 2 displays the SEM micrographs of raw magnesite ore, showing its surface morphology. The ore has an uneven surface texture, most likely due to gas release during weathering and formation. Magnesite is the primary constituent of the sample, with varying concentrations of quartz. The sample also contains small veinlets of dolomite. In magnesite within the shear zones, euhedral dolomite and calcite crystals were observed. The XRF analysis of the Magnesite sample reveals that it mainly comprises magnesite with some subordinate minerals. The sample contains 37.68% MgO, 7.24% CaO, 3.10% SiO_2, 1.91% Fe_2O_3, 0.58% Al_2O_3, and 48.65% LOI. Table 2 shows the weight percentage, the chemical analysis, and the distribution of Fe_2O_3 in each fraction size. The (-0.212+0.05mm) fraction size has the highest weight and iron impurities distribution, accounting for 54.45% and 56.03%, respectively. The (-0.63+0.212mm) fraction size also contains significant iron impurities. However, the (-0.05 mm) fraction size has a minor yield and iron impurities. Despite this, the slimes (-0.05mm) have lower iron impurities and could potentially improve the overall product quality. However, managing slimes presents a major challenge due to their low mass, large surface area, and high surface energy, which ultimately decreases the efficiency of the mineral separation process (Ansari, 1997). Therefore, the parameter optimization process will not include the slimes.

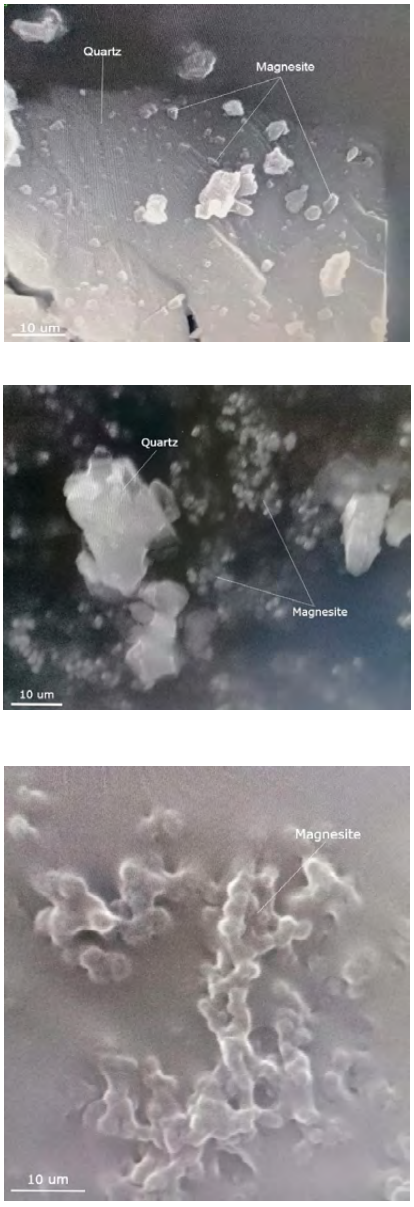

Figure 2. *Photomicrographs of Saudi magnesite sample*

Table 2. Chemical analysis of iron impurities by XRF of each fraction size of magnesite sample

Particle size (mm)	Weight %	Fe_2O_3%	Distribution of Fe_2O_3
-0.63+0.425	16.23	1.89	16.09
-0.425+0.212	21.08	1.83	20.23
-0.212+0.1	37.91	1.98	39.37
-0.1+0.05	16.54	1.92	16.66
-0.05	8.24	1.77	7.65
Total	100.00	1.89	100

3.2 Dry High-Intensity Magnetic Separation (DHIMS)

Effect of the feed size

Figure 3 displays the test results for the effect of feed size on the yield, recovery, and assay of non-magnetic material. Notably, there were no significant changes in non-magnetic yield. The recovery and assay decrease consistently from 80.32% and 1.85% to 49.67% and 1.32%, respectively, as the feed size decreases. However, as feed size becomes finer, recovery and assay increase again to 57.94% and 1.46%, respectively. As per the findings, the separation effectiveness was directly proportional to the reduction in particle size, and the liberation between magnesite and impurities increased as it reached its optimal size of (-0.212+0.05mm). However, the separation efficiency declined as the feed size became finer. The iron impurity assay significantly improved, reducing from 1.85% to 1.32%. These results align with previous research that employed feed sizes similar to the identified optimum size. (Ignjatović et al., 1995; Yehia & Al-Wakeel, 2013).

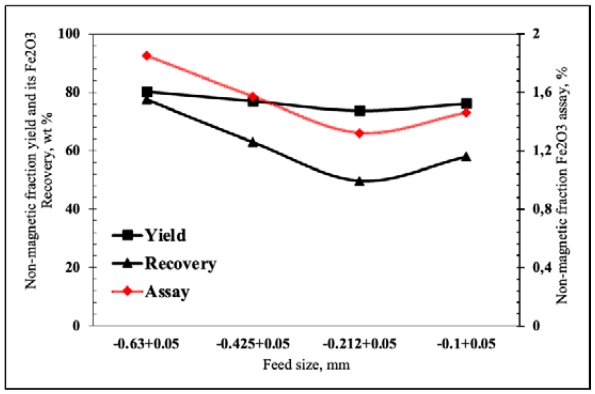

Figure 3. *Effect of the feed size on the non-magnetic material's yield and iron impurities (Fe_2O_3)'s recovery and assay*

Effect of the feed rate

The results of the impact of feed rate on yield, recovery, and assay of non-magnetic material are shown in Figure 4. As the feed rate increased from 0.3kg/min to 1.2kg/min, all three components experienced an increase. Specifically, the yield of non-magnetic material rose from 72.82% to 80.66%, while the recovery and assay of iron impurities also increased from 43.23% and 1.15% to 67.45% and 1.62%, respectively. a rise in feed rate results in reduced residence time in the magnetic field, ultimately leading to decreased selectivity during the separation process. On the other hand, a feed rate of 0.3kg/min was found to be the most effective due to the extended exposure to the magnetic field (Naik, 2002).

Effect of the magnetic field

The outcomes of tests that investigate the impact of a magnetic field on the yield, recovery, and assay of non-magnetic substances are presented in Figure 5. The non-magnetic yield remains unchanged, but the recovery and assay of iron impurities indicate that the separation efficiency enhances as the magnetic field

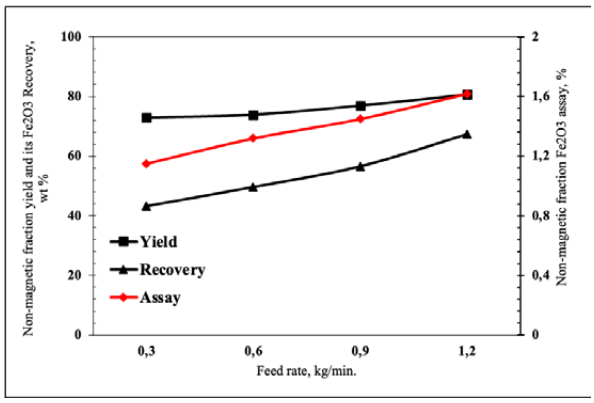

Figure 4. *Effect of the feed rate on the non-magnetic material's yield and iron impurities (Fe_2O_3)'s recovery and assay*

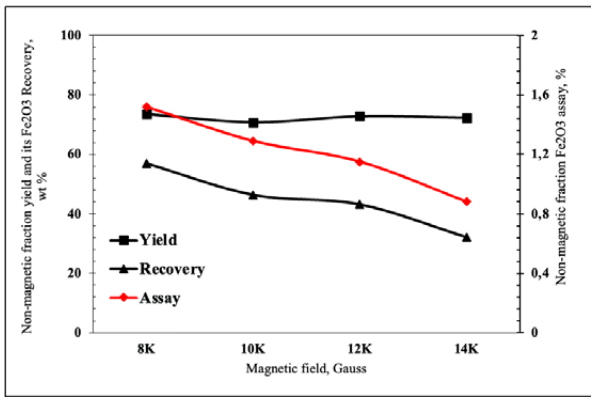

Figure 5. *Effect of the magnetic field on the non-magnetic material's yield and iron impurities (Fe_2O_3)'s recovery and assay*

strength increases. There was a gradual improvement in the recovery and assay of iron impurities from 8K to 12K Gauss, resulting in a 13.71% decrease in recovery and a 0.37% decrease in the assay. When the magnetic field was increased to 14K Gauss, there was a rapid improvement in both recovery and assay, and the yield of non-magnetic material remained stable. This enhancement resulted in a 10.99% increase in recovery and a 0.27% increase in the assay.

Effect of the roll speed

The impact of roll speed on the yield, recovery, and assay of non-magnetic material are depicted in Figure 6. The data indicates a slight improvement in recovery and assay occurred as the roll speed increased from 30 to 40 rpm. However, it was at 50 rpm that a significant improvement in removing iron impurities was observed. The iron removal rate improved from 56.77% to 72.32%, and the assay rate went from 1.15% to 0.71%. It is worth noting that increasing the speed beyond this point decreased the separation efficiency due to increased centrifugal forces acting on the particles, which can affect their adherence and release behavior (Yehia & Al-Wakeel, 2013). The product can be utilized in various industries, including chemical,

fertilizer, and wastewater treatment, as well as flue gas treatment and pesticides (J. et al. et al., 2020; Guo et al., 2013; Jandl et al., 2001; Tian et al., 2021).

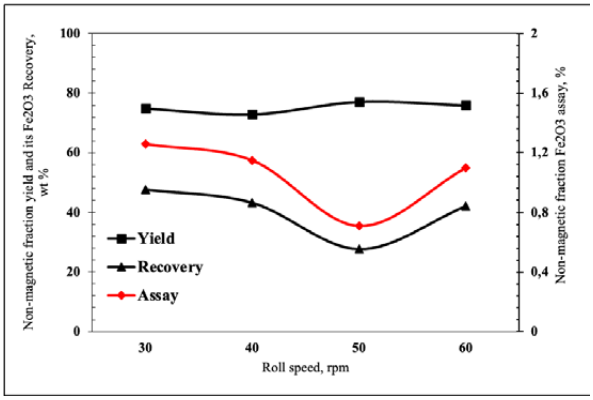

Figure 6. *Effect of the roll speed on the non-magnetic material's yield and iron impurities (Fe_2O_3) recovery and assay*

3.3 Wet High-Intensity Magnetic Separation (WHIMS)

Effect of the flow rate

Figure 7 displays the effects of flow rate on the yield, recovery, and assay of non-magnetic material. The findings indicate that the yield remained relatively stable as the flow rate increased from 0.4 to 1.6 L/min, with the highest yield of approximately 71.82% at 1.6 L/min and the lowest yield of approximately 65.36% at 0.4 L/min. However, with a decrease in flow rate, there was an increase in the amount of iron impurities captured. A flow rate of 0.4 L/min appeared to have the most favorable outcome concerning iron assay and recovery, showing a better result by 1.18% and 39.38%, respectively. On the other hand, a flow rate of 1.6 L/min led to the poorest results in terms of iron impurities assay and recovery, with an increase of 1.34% and 49.16%, respectively. This is because a slower flow rate allowed a greater exposure to the magnetic field, leading to higher separation efficiency and a lower assay of iron impurities in the non-magnetic material (TAÇOĞLU et al., 2021).

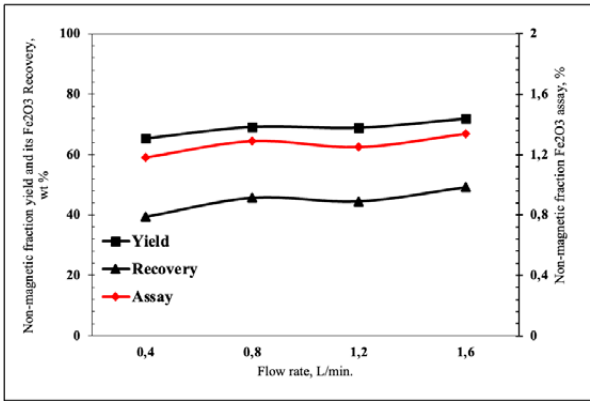

Figure 7. *Effect of the flow rate on the non-magnetic material's yield and iron impurities (Fe_2O_3) recovery and assay*

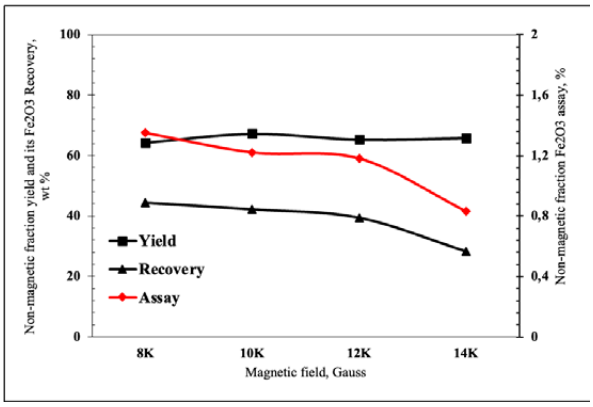

Figure 8. *Effect of the magnetic field on the non-magnetic material's yield and iron impurities (Fe_2O_3) recovery and assay*

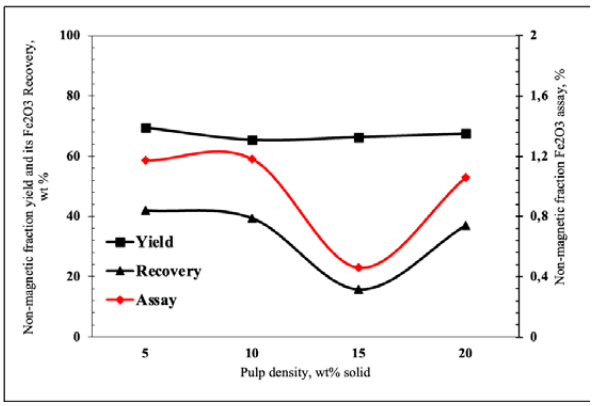

Figure 9. *Effect of the magnetic field on the non-magnetic material's yield and iron impurities (Fe_2O_3) recovery and assay*

Effect of the magnetic field

Figure 8 presents the effect of magnetic fields on the yield, recovery, and assay of non-magnetic materials. The outcomes indicate that the yield remained steady as the magnetic field increased from 10K to 14K Gauss, with a slight dip noted at 8K Gauss. With the rise in magnetic field intensity from 8K to 14K Gauss, a decrease occurred in the concentration of iron impurities and recovery, from 1.35% and 44.37% to 0.83% and 28.23%, respectively. The rapid decrease seen during dry magnetic separation was also observed in wet magnetic separation, between 12K and 14K Gauss.

Effect of the pulp density

Figure 9 illustrates the results of the impact of pulp density on the yield, recovery, and assay of non-magnetic materials. Based on the outcomes, it can be inferred that the yield remained consistent as the pulp density escalated from 5 to 20 wt.% solid, with a minor upsurge observed at 5 wt.% solid. The iron content of the concentration remained consistent, but there was a slight 2.63% decrease in recovery when the pulp density was increased to 10 wt.% solid. Subsequently, there was a significant decline in both iron content and recovery, dropping from 1.18% and 39.38% to 0.46% and 15.75%,

respectively. As the pulp density continued to increase, separation efficiency decreased, while iron content and recovery increased to 1.06% and 37.05%. Lowering the pulp density results in increased pulp velocity, which, unfortunately, reduces particle capture and recovery. Conversely, raising the pulp density can overcrowd the matrix and limit recovery capability (Makhula et al., 2016). The product can be used in refractory materials, brake lining industry, leather treatment, and welding industry (Zhang & Duan, 2020, de Sousa, 2018; Haferkamp et al., 2003; Yuvaraj et al., 2020)

CONCLUSION

The results of the investigation conducted on low-grade Saudi magnesite ore indicate that WHIMS is more effective than DHIMS in reducing iron impurities. The study identified that the optimal conditions for WHIMS were the magnetic field of 14K Gauss, the solid feed of 15 wt.%, and a flow rate of 0.4 L/min. These conditions resulted in a product that showed only 0.46% Fe_2O_3, which is a remarkable 84.25% removal of iron. The DHIMS process was able to remove up to 72.32% of iron successfully. This was achieved with DHIMS parameters at the feed size of (-0.212+0.05mm), flow rate of 0.3 kg/min, magnetic field strength of 14 KGauss, and roll speed of 50 rpm. The resulting product had a concentration of 0.71% Fe_2O_3.

REFERENCES

1. Atasoy, A. (2019). The wet high intensity magnetic separation of magnesite ore waste. Hemijska Industrija, 73(5), 337–346.
2. Bentli, I., Erdogan, N., Elmas, N., & Kaya, M. (2017). Magnesite concentration technology and caustic–calcined product from Turkish magnesite middlings by calcination and magnetic separation. Separation Science and Technology, 52(6), 1129–1142.
3. Biswas, S., & Sarkar, D. (2020). Introduction to Refractories for Iron-and Steelmaking. Springer.
4. Chatterjee, K. K. (2009). Uses of industrial minerals, rocks and freshwater. Nova Science Publishers.
5. Chatterjee, K. K. (2013). Uses of industrial mineals, rocks and freshwater. In Nova Science Publishers, In (Vol. 53, Issue 9).
6. Chen, J. L., Gao, L., Jiang, Q., Hou, Q., Hong, Y., Shen, W., Wang, Y., & Zhu, J. H. (2020). Fabricating efficient porous sorbents to capture organophosphorus pesticide in solution. Microporous and Mesoporous Materials, 294, 109911.
7. de Sousa, M. F. (2018). Magnesium oxide: A Forgotten Specialty Chemical.
8. Dippenaar, R. (2005). Industrial uses of slag (the use and re-use of iron and steelmaking slags). Ironmaking & Steelmaking, 32(1), 35–46.
9. Guo, H., Xie, J., Hu, H., Li, X., Fan, T., Nan, H., & Liu, Y. (2013). Preparation of lamellar Mg (OH) 2 with caustic calcined magnesia through apparent hydration of MgO. Industrial & Engineering Chemistry Research, 52(38), 13661–13668.
10. Haferkamp, H., Ostendorf, A., Bunte, J., Cordini, P., & Meier, O. (2003). 509 Laser Beam Welding of Magnesium Alloys A Process at the Threshold to Industrial Manufacturing. Proceedings of International Conference on Leading Edge Manufacturing in 21st Century: LEM21 2003, 891–896.
11. Hou, Q., Luo, X., Xie, Z., Li, Y., An, D., & Li, J. (2020). Preparation and characterization of microporous magnesia- based refractory. International Journal of Applied Ceramic Technology, 17(6), 2629–2637.
12. Hredzak, S., Matik, M., Lovas, M., Znamenackova, I., Stefusova, K., & Zubrik, A. (2015). Separability of Calcined Magnesite Fines in Magnetic Field. Inżynieria Mineralna, 16(2), 183–188.
13. Ignjatović, M. R., Ćalić, N., Marković, Z. S., & Ignjatović, R. (1995). Development of a Combined Gravity–Magnetic Sepaitation Process for Magnesite ORE Using HGMS. Physical Separation in Science and Engineering, 6, 161–170.
14. ISHIHARA, S., TERASHIMA, S., & TSUKIMURA, K. (1987). Spatial Distribution of Magnetic Susceptibility and Ore Elements, and Cause of Local Reduction on Magnetite-series Granitoids and Related Ore Deposits at Chichibu. Mining Geology, 37(201), 15–28. https://doi.org/10.11456/shigenchishitsu1951.37.15
15. Jandl, R., Glatzel, G., Katzensteiner, K., & Eckmüllner, O. (2001). Amelioration of magnesium deficiency in a Norway spruce stand (Picea abies) with calcined magnesite. Water, Air, and Soil Pollution, 125(1), 1–17.
16. Jung, I.-H., Decterov, S. A., & Pelton, A. D. (2005). Critical thermodynamic evaluation and optimization of the CaO–MgO–SiO2 system. Journal of the European Ceramic Society, 25(4), 313–333.
17. Kandianis, F., & Kandianis, V. (2002). High-Purity Dead Burned Magnesia. Industrial Minerals, 421, 40–41.
18. Kim, D.-Y., Pyeon, S.-J., Lim, J.-J., & Lee, S.-S. (2018). Strength properties of inorganic adhesives using dead burned magnesia and phosphate according to addition ratio of borax. Proceedings of the Korean Institute of Building Construction Conference, 48–49.
19. Li, C., Sun, C., Wang, Y., Fu, Y., Xu, P., & Yin, W. (2020). Research on new beneficiation process of low-grade magnesite using vertical roller mill. International Journal of Minerals, Metallurgy and Materials, 27, 432–442.
20. Makhula, M. J., Falcon, R. M. S., Bergmann, C. P., & Bada, S. O. (2016). Statistical analysis and concentration of iron ore using Longi LGS 500 WHIMS. International Journal of Mining Science and Technology, 26(5), 769–775.
21. Naik, P. K. (2002). Quantification of induced roll magnetic separation of mineral sands. Scandinavian Journal of Metallurgy, 31(6), 367–373.
22. Rudnykh, T. G., Nikolaeva, L. M., Mezentsev, E. P., Chistyakov, Y. N., & Kirillov, L. P. (1988). Influence of the impurity concentrations of rocks in original

magnesites on the quality of the raw materials and concentrates. Refractories, 29(5), 289–294.
23. Shand, M. A. (2006). The chemistry and technology of magnesia. John Wiley & Sons.
24. Suvorova, D. I., Potapenko, V. E., Tyuryukhanova, V. V, Mezentsev, E. P., & Kryuchkov, V. A. (1984). A method of production of magnesite powder of the 3-1-mm fraction by magnetic separation. Refractories, 25(11–12), 696–698.
25. TAÇOĞLU, M. E., Mustafa, Ş. E. N., TOPRAK, E., & SAKLAR, S. (2021). The Effect of Water Flow Rate on Davis Tube Tests. Geosound, 54(1), 44–53.
26. Tian, H., Wan, D., Che, Y., Chang, J., Zhao, J., Hu, X., Guo, Q., Wang, Z., & Wang, L. (2021). Simultaneous magnesia regeneration and sulfur dioxide generation in magnesium-based flue gas desulfurization process. Journal of Cleaner Production, 284, 124720.
27. Wang, Q. Q., Li, X. A., Wei, D. Z., & Dai, S. J. (2011). The Application of Magnesite Processing Technics. Applied Mechanics and Materials, 71, 2323–2326.
28. Wu, W., Yang, Q., Qi, G. A. O., & Zeng, J. (2020). Effects of calcium ferrite slag on dephosphorization of hot metal during pretreatment in the BOF converter. Journal of Materials Research and Technology, 9(3), 2754–2761.
29. Xue, P., He, D., Xu, A., Gu, Z., Yang, Q., Engström, F., & Björkman, B. (2017). Modification of industrial BOF slag: Formation of MgFe2O4 and recycling of iron. Journal of Alloys and Compounds, 712, 640–648.
30. Yehia, A., & Al-Wakeel, M. (2013). Role of ore mineralogy in selecting beneficiation route for magnesite-dolomite separation. Physicochemical Problems of Mineral Processing, 49.
31. Yehia, A., & Al-Wakeel, M. I. (2000). Talc separation from talc-carbonate ore to be suitable for different industrial applications. Minerals Engineering, 13(1), 111–116.
32. Yuvaraj, A., Karmegam, N., Ravindran, B., Chang, S. W., Awasthi, M. K., Kannan, S., & Thangaraj, R. (2020). Recycling of leather industrial sludge through vermitechnology for a cleaner environment—A review. Industrial Crops and Products, 155, 112791.
33. Zhang, Y., & Duan, X. (2020). Chemical precipitation of heavy metals from wastewater by using the synthetical magnesium hydroxy carbonate. Water Science and Technology, 81(6), 1130–1136.